Nanosatellites Formation Flying Control Approaches Overview

Danil Ivanov, Mikhail Ovchinnikov, Stepan Tkachev

Keldysh Institute of Applied Mathematics RAS, Miusskaya sq. 4, Moscow, Russia

danilivanovs@gmail.com

Abstract. The paper considers various approaches nanosatellites formation flying control , presents dynamic models of the motion of a group of nanosatellites, considers various algorithms for controlling relative angular and translational motions, taking into account the specifics of small satellites and limited inter-satellite communication capabilities. The paper discusses various approaches to the formation flying control, including those using perspective methods that do not require the fuel consumption. With a large number of spacecraft in a group, a new class of space systems appears, defined as a swarm. The main difficulty in implementing a swarm formation flying of satellites is navigation and control of the mutual relative motion of an individual satellite in a swarm, taking into account the fundamental impossibility of having information about the phase state vector of each swarm element. The features of decentralized algorithms for controlling the satellites swarm motion are considered and the dynamics of the swarm is investigated.

1. Introduction

To solve modern fundamental and applied problems in near-earth space, distributed multi-element space systems are increasingly used. As a rule, these are several spacecraft moving at a short relative distance, which are combined into a single system and work to achieve a common goal. Due to the limited budget for missions with a large number of satellites for the construction of distributed systems, small satellites are considered that have several restrictions on mass, size, energy, on-board computing power and the composition of the control system equipment. This leads to the complication of onboard control algorithms for the main modes of motion at the stage of mission design, taking into account the constrained capabilities of the satellites. The construction of multi-element satellite systems requires specialized dynamic models, special algorithms for identifying the current phase state and controlling the orbital and angular motion of vehicles, which is caused by the above restrictions.

There are two main approaches to the autonomous control of a group of satellites: centralized control and decentralized control. Centralized control implies the presence of a "head" or "mother" satellite in the formation, its motion is monitored by the remaining "deputy" or "daughter" satellites that are controlled to achieve the required relative trajectories. Centralized control is more suitable for small groups of satellites moving along predetermined relative trajectories. For a significant number of satellites like the swarm, this approach seems to be not reasonable since the head satellite may be beyond the communication range for some satellites. Additionally, inter-satellite communication always has a limited number of channels. This makes it difficult to determine the motion of the

"mother" satellites relative to the "daughters". With the decentralized control approach, each satellite makes the decision to control its dynamic states, modes, and activities individually based on the information on motion of the nearest neighbors. This approach is more suitable for a swarm of satellites taking into account the communicational limitations.

The conventional approach to formation flying is to use onboard propulsion for producing the required force to control relative position in the formation. To be able to implement a given thrust direction, a three-axis attitude control system must also be installed onboard. Such systems with full controllability are often used on satellites of a large size and mass, and a large number of different control algorithms have been developed for these large-scale missions [1–3]. As has been previously noted the nanosatellite ability to perform any maneuvers are restricted due to mass, cost, and volume constraints. There could be no propulsion system onboard at all. That is why in this paper we will focus on fuelless control approaches.

1. Relative motion equations

To explain the relative motion often used Clohessy-Wiltshire equation. They are linearized equation of motion, from which the exact solutions for specific parameters can be obtained to construct the configuration of various formations. This equations describe the relative motion of two satellites flying in the near circular orbits in the central gravitational field. The orbital reference frame is used, its origin (reference point) moves along the circular orbit of radius r_0 with the orbital angular velocity $\omega = \sqrt{\mu / r_0^3}$ where μ is the Earth gravitational parameter. Axis Oz is aligned along the vector from the center of the Earth to the reference point, axis Oy is directed along the normal to the orbital plane, axis Ox complements the reference frame to the right-handed one (Figure.1).

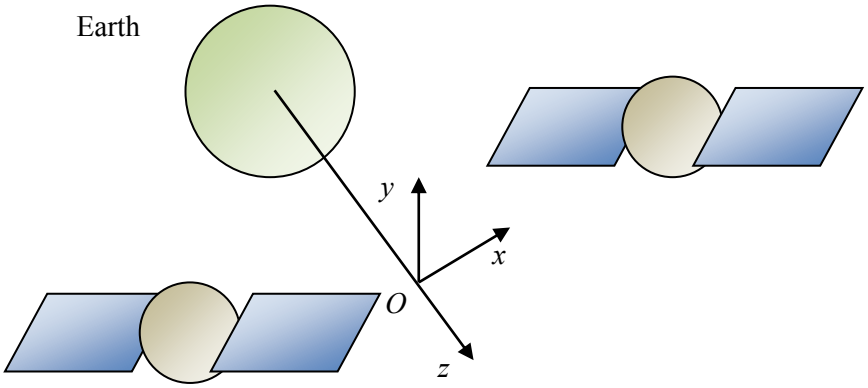

Figure 1. Reference frame associated with the point O moving along the circular orbit

Let $\mathbf{r}_1 = (x_1, y_1, z_1)$ and $\mathbf{r}_2 = (x_2, y_2, z_2)$ be the radius-vectors of the first and second satellites in ORF. Then the components of the relative position vector $\mathbf{r} = \mathbf{r}_2 - \mathbf{r}_1 = (x, y, z)$ are governed by the following equations

$$\begin{aligned} \ddot{x} &= -2\dot{z}\omega + u_x, \\ \ddot{y} &= -y\omega^2 + u_y, \\ \ddot{z} &= 2\dot{x}\omega + 3z\omega^2 + u_z \end{aligned} \tag{1}$$

where $\mathbf{u} = \begin{bmatrix} u_x & u_y & u_z \end{bmatrix}^T$ is the control vector. In the case of free motion, i.e. if $\mathbf{u} = 0$, the exact solution of (1) is

$$
\begin{aligned}
x(t) &= -3C_1\omega t + 2C_2\cos\omega t - 2C_3\sin\omega t + C_4,\\
y(t) &= C_5\sin\omega t + C_6\cos\omega t,\\
z(t) &= 2C_1 + C_2\sin\omega t + C_3\cos\omega t
\end{aligned}
\qquad (2)
$$

where the constants $C_1, C_2, C_3, C_4, C_5, C_6$ are defined by the initial conditions. The term responsible for the relative drift is $-3C_1\,\omega t$. The relative trajectory of two satellites is closed if and only if $C_1 = 0$. However, ideal initial conditions for a closed free motion cannot be achieved. Moreover, perturbations and nonlinear effects induce additional relative drift between the satellites. Therefore, the satellites must be controlled to eliminate the drift and to achieve the bounded relative trajectory. The term C_4 is responsible for the displacement of the center of the instant ellipse in the along-track direction. The instant ellipse is the trajectory that can be obtained from (2) with zero relative drift. C_4 values can be referred to as relative shifts. Specific distribution of the satellite in the swarm requires C_4 values control. Examples of the relative trajectories demonstrating the relative shift and relative drift are presented in Figure 2.

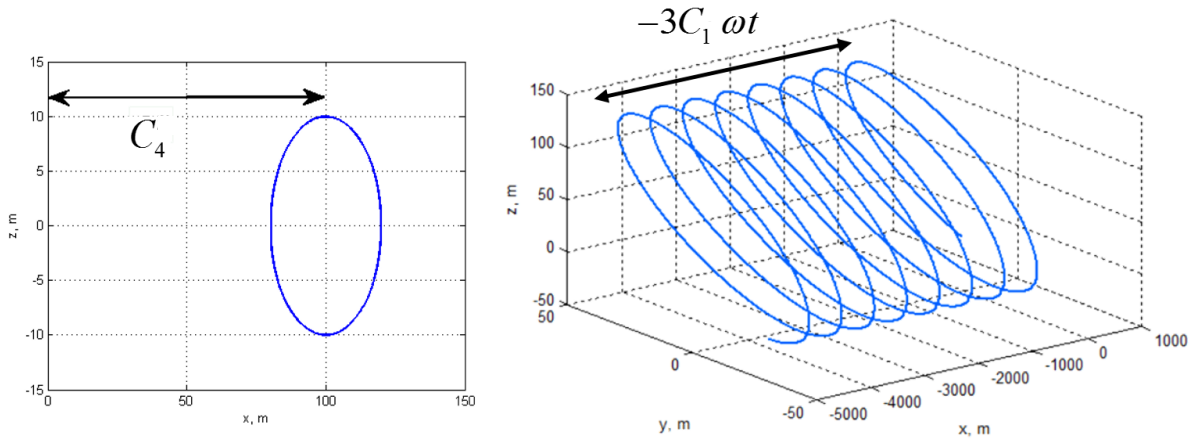

Figure 2. Trajectories describing the relative shift C_4 and the relative drift $-3C_1\,\omega t$

In the common case the nanosatellite formation flying are controlled in order obtain certain relative configuration, that can be explained by the constants in the equations (1). Consider a set of control approaches that can be applied for the set of tasks.

2. Control forces models

2.1. Environmental forces

The use of environmental forces for formation flying motion control is an attractive idea [4]. Environmental forces, such as aerodynamic drag (AD) force [5–9] and solar radiation pressure (SRP) force [10–14], can be used. First of all, one might solve a problem of station keeping and reconfiguration without any propellant. Second, both approaches require a sail or form-factor of satellites with high area-to-mass ratio. The CubeSats of 3U size are already appropriate for differential drag application. The principal idea here is to use a difference in environmental forces acting on each satellite in formation flying. This difference usually appears when the satellite changes its relative attitude but the effective size variation is also considered in the literature. Though in general the AD and SRP acceleration models are similar, there are a number of differences. One can apply AD control in low-Earth orbits (LEO) only, and its value is varying due to the atmosphere density change caused by the day\night variations and the orbital altitude variations. So, it is usually difficult to predict the

exact value of the control force. SRP can be used in different types of orbits but the shaded parts of orbit should be taken into consideration.

The model of the aerodynamic drag force f_i acting on the i-th satellite can be represented in the following form:

$$f_i = -\frac{1}{2} C_a \rho V_o^2 \Delta S \sin \alpha_i - \frac{1}{2} C_a \rho V_o^2 S_0 \tag{3}$$

where C_a is the aerodynamic drag coefficient, ρ is the density of the atmosphere, V_o is the velocity of the incoming airflow, ΔS is the difference between the maximum and minimum values of the cross-section area of the satellite, S_0 is the minimum value of the cross-sectional area of the satellite, $\alpha_i \in [0; \pi/2]$ is the angle between the direction of the incoming airflow and the longitudinal axis of satellites that are assumed to be axisymmetric.

The physical processes of the interaction of the atmospheric particles with the satellite surface are complex. Assume that the interaction proceeds mechanically through two schemes – a mirror one, when the reflection of the molecule from the surface is absolutely elastic, and diffuse one in the case of an absolutely inelastic collision.

$$\mathbf{f}_i = -\frac{1}{m} \rho V^2 S \left\{ (1-\varepsilon)(\mathbf{e}_V, \mathbf{n}_i)\mathbf{e}_V + 2\varepsilon(\mathbf{e}_V, \mathbf{n}_i)^2 \mathbf{n}_i + (1-\varepsilon)\frac{\upsilon}{V}(\mathbf{e}_V, \mathbf{n}_i)\mathbf{n}_i \right\}. \tag{4}$$

Here ρ is the atmosphere density, m is the satellite mass, V is the airflow velocity, S is the plate area, $\mathbf{n}_i$ is the unit vector of the normal to the plate, $\mathbf{e}_V$ is a unit vector directed along the velocity of the incoming airflow, ε is the coefficient of reflected molecules, υ is a parameter proportional to the most probable thermal velocity of the diffusely reflected molecules, $i = 1, 2$. The first term in (4) determines the aerodynamic drag force directed against the velocity of the air flow. The second and third terms are the force components directed against the normal to the plate, which define the lift force.

The SRP acceleration is written as follows (see [4]):

$$\mathbf{f}_{SRP} = \frac{PS}{m}(\mathbf{s}, \mathbf{n}) \left((1 - \rho_s - \rho_t)\mathbf{s} + \left(2\rho_s (\mathbf{s}, \mathbf{n}) + \frac{2}{3}\rho_d \right) \mathbf{n} \right) \tag{5}$$

Here $(\mathbf{s}, \mathbf{n}) = \cos\alpha$ means the dot product of the unit vector $\mathbf{s}$ from the Sun and the normal to the sail $\mathbf{n}$, P is the nominal solar radiation pressure constant at a distance of 1 astronomical unit from the Sun, and ρ_t, ρ_s, ρ_d are the fractions of photons transmitted, specularly reflected, and diffusively reflected, respectively.

2.2. Electrostatic and electromagnetic formation control

A concept of electrostatic formation flying control was suggested in [15]. This concept is based on the SCATCHA mission [16] where the satellite electrostatic charge system was tested. The following papers [17–26] developed this idea. The thing one should start with is the two satellites interaction force [18,19,21]

$$\mathbf{F}_{ij} = k_c \frac{\mathbf{r}_{ij}}{r_{ij}^3} q_i q_j e^{-\frac{r_{ij}}{\lambda_d}} \left(1 + \frac{r_{ij}}{\lambda_d} \right). \tag{6}$$

Here $\mathbf{r}_{ij}$ is the radius vector from i-th to j-th satellite, q_i and q_j are their charges, k_c is the Coulomb interaction constant, and λ_d is the environment Debye length.

The similar concept is the electromagnetic formation flying. It includes the control via electromagnetic field which is produced by the magnetic coils installed on each satellite in formation.

This approach was carefully studied in [27]; further studies were carried out in [28–34]. For this case, the so-called far-field model is derived in [27]

$$\mathbf{F}_{ij} = -\frac{3\mu_0}{4\pi}\left(-\frac{\left(\boldsymbol{\mu}_i, \boldsymbol{\mu}_j\right)}{d_{ij}^5}\mathbf{d}_{ij} - \frac{\left(\boldsymbol{\mu}_i, \mathbf{d}_{ij}\right)}{d_{ij}^5}\boldsymbol{\mu}_2 - \frac{\left(\boldsymbol{\mu}_j, \mathbf{d}_{ij}\right)}{d_{ij}^5}\boldsymbol{\mu}_1 + 5\frac{\left(\boldsymbol{\mu}_i, \mathbf{d}_{ij}\right)\left(\boldsymbol{\mu}_j, \mathbf{d}_{ij}\right)}{d_{ij}^7}\mathbf{d}_{ij} \right) \quad (7)$$

where $\boldsymbol{\mu}_i$ and $\boldsymbol{\mu}_j$ are the satellite magnetic dipoles and $\mathbf{d}_{ij}$ is the vector from the center of i-th coil to the center of j-th one.

The use of the Lorentz force should be noted. This idea is another way to use the satellite electrostatic charge [35–37]. An expression for the force in this concept is the following

$$\mathbf{F}_L = q\left(\mathbf{V}_{orb} - \boldsymbol{\Omega}_E \times \mathbf{r}\right) \times \mathbf{B} \quad (8)$$

Here $\mathbf{r}$ and $\mathbf{V}_{orb}$ is the satellite position and orbital velocity, respectively, and $\boldsymbol{\Omega}_E$ is the Earth's angular velocity, $\mathbf{B}$ is the geomagnetic field vector. Unlike the electrostatic control, this force can be used only in LEO due to decreasing $\mathbf{B}$ when the orbital altitude increases. From (8), one can see that there is only one control input q for each satellite. The electrostatic interaction between the satellites can be neglected as λ_d is extremely low in LEO.

2.3. Some other fuelless control approaches

The concept of tethered satellites formation flying can also be implemented using CubeSats. The main idea is to link two or more satellites by some rope and to control the relative motion by changing its length [38–41]. The realization of this concept is complicated because of flexible rope motion [42]. So, the relative motion of the two connected by tether satellites is usually designed to provide the tension of the tether.

Another approach involves system total momentum conservation. The main idea here is that each satellite can inject some mass but, unlike the case of ordinary thrusters, other satellites in a formation can catch this mass. The concept was studied in [43,44]. In [45], this idea was examined in the case when the satellites can produce and consume the stream of small liquid droplets. In [46], the satellites overthrew one object. It seems that this concept is the most exotic way of relative motion control, and its application is quite difficult from the engineering point of view.

3. Control algorithms

According to the equations of relative free motion in the common case of two satellites flying at close distances, the satellites will move along in an un-bounded elliptical spiral relative trajectory. That is why the relative motion control is needed for keeping close formation flight. The control in formation flying can be used for various tasks: tracking or maintenance of the required relative motion, reconfiguration, proximity operations and even docking to each other. This section describes the main features of nanosatellite formation flying control.

A large number of papers applied a variety of the different formation flying control algorithms: PID regulators [47], linear-quadratic regulators (LQR) [48], Lyapunov-based control [49,50], sliding mode control [51], optimal control [52] etc. In the paper we demonstrate application of LQR and Lyapunov-based control in centralized and decentralized strategies for different tasks using different control forces.

3.1. LQR-based control

Consider an example of the centralized aerodynamic based control using aerodynamic force model (4). Let the satellites be also equipped with the reaction wheel-based attitude control system [53]. It provides the attitude to produce the required aerodynamic force. The control goal is to achieve the desired relative trajectory defined by the free relative motion according to (1). The feedback control algorithm based on LQR is developed under these assumptions.

Rewrite (1) in the matrix-vector form

$$\dot{\mathbf{x}} = A\mathbf{x} + B\mathbf{u} \tag{9}$$

where $\mathbf{x} = [\mathbf{r}^T \ \mathbf{v}^T]^T$ is the state vector, A is the dynamic matrix

$A = \begin{bmatrix} 0_{3x3} & E \\ C & D \end{bmatrix}$, E is the identity matrix with size 3x3,

$$C = \begin{bmatrix} 0 & 0 & 0 \\ 0 & -\omega^2 & 0 \\ 0 & 0 & 3\omega^2 \end{bmatrix}, \ D = \begin{bmatrix} 0 & 0 & -2\omega \\ 0 & 0 & 0 \\ 2\omega & 0 & 0 \end{bmatrix},$$

B is the control matrix

$$B = \begin{bmatrix} 0_{3x3} \\ E \end{bmatrix},$$

$\mathbf{u}$ is the control vector. For the formation flying controlled by the differential aerodynamic force the control vector $\mathbf{u} = \Delta\mathbf{f}$.

The desired relative motion corresponds to the free motion of the system described by the equation

$$\dot{\mathbf{x}}_d = A\mathbf{x}_d$$

where $\mathbf{x}_d$ is the desired state vector. Then one can obtain linear equation of the dynamics of the deviation from the desired trajectory

$$\dot{\mathbf{e}} = A\mathbf{e} + B\mathbf{u} \tag{10}$$

where $\mathbf{e} = [\mathbf{x}^T - \mathbf{x}_d^T]^T$.

Linear quadratic regulator is the feedback control $\mathbf{u} = K\mathbf{e}$ which ensures the minimum of the functional

$$J = \int_0^\infty (\mathbf{e}^T Q\mathbf{e} + \mathbf{u}^T R\mathbf{u})dt \tag{11}$$

along the trajectory [54]. Here Q, R are the positive definite matrices that determine the weight of errors for the state vector and the weight of the control resource consumption respectively.

The feedback minimizing the functional is determined by the equation

$$\mathbf{u} = -R^{-1}B^T P\mathbf{e} \tag{12}$$

where the matrix P is obtained as a solution of the Riccati equation

$$A^T P + PA - PBR^{-1}B^T P + Q = 0. \tag{13}$$

Consider an example of the application of the LQR-based control algorithm [48]. One of the satellites moves in a low-earth circular orbit with the altitude $h = 340$ km. Another satellite moves at a

short distance. The night time density of the atmosphere is approximately $\rho \approx 10^{-11}\ \mathrm{kg/m^3}$. Figure 2 provides the initial, reference and controlled relative orbits. The relative trajectory of the satellites is gradually converging to the reference orbit. It should be noted that the aerodynamic force cannot implement the calculated by (12) control, so in the simulation of motion this restrictions is taken into account.

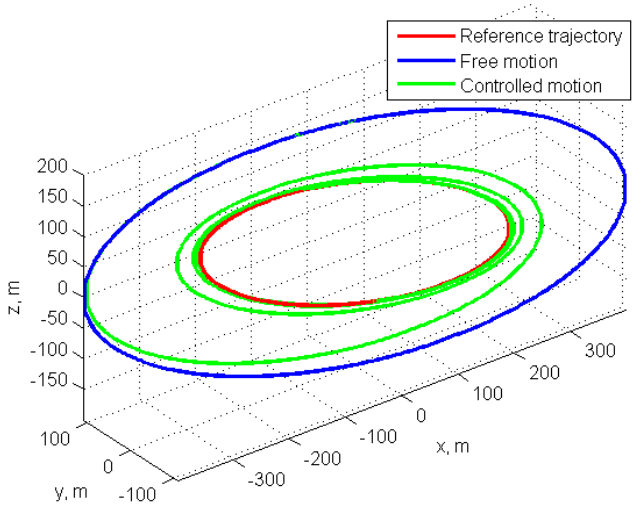

Figure 2. Relative reference trajectory and controlled motion using aerodynamic forces

The presented in Figure 2 control is applied in the centralized coordinated manner when one satellite is controlled in accordance with other satellite motion. The centralized control implies the presence of a head satellite in the formation, its motion is monitored by the remaining satellites, which are controlled to achieve the required relative trajectory, or the head satellite sends the control commands to the other satellites. On the contrary, the decentralized control approach means that each satellite is controlled individually and independently based on the relative motion. It is assumed that the calculated control applied to the other satellites could be unknown.

Consider a decentralized control with the use of differential lift and drag for constructing satellite formation flying in the shape of a required configuration. Each satellite in the formation is equipped with a sunlight reflector. In the appropriate lighting conditions such formation can be visible from Earth and provide graphic images in the sky. The main problem of the LQR application to the multi-satellite formation is that for each of the *N* satellites there are *N-1* desired trajectories relative to each of the rest of the satellites. The desired relative trajectories are chosen in the way that all the satellites are located in the spots corresponding to the respective pixels of the letters-to-be-displayed during the motion. So, each satellite needs to apply the control (12) for each trajectory deviation. But the deviations $\mathbf{e}_{ij}$ could lead to the completely different control vectors $\mathbf{u}_{ij}$. That is why a strategy has to be defined for the constructing of the required formation.

We propose the following scheme to solve this problem. For each satellite one can calculate the mean vector of the deviations $\bar{\mathbf{e}}_i$ as follows:

$$\bar{\mathbf{e}}_i = \sum_{j=1}^{N-1} \mathbf{e}_{ij} \,/\, (N-1)\,,$$

Then, using (12), the control vector is calculated:

$$\bar{\mathbf{u}}_i = -R^{-1} B^T P \bar{\mathbf{e}}_i\,. \qquad (14)$$

Thus, the relative trajectory of the i-th satellite will converge to some average desired relative trajectory, but in the end all of the relative deviations will decrease and the required image configuration will be obtained. The Figure 3 shows the relative trajectories of 75 CubeSats with Sun reflectors that is achieved after the cluster launch to form letters «ИПМ» for the Keldysh Institute of Applied Mathematics RAS. The construction of the required configuration with given parametes took about 25 hours on the orbit with 350 km of altitude and 2x2 m Sun reflectors.

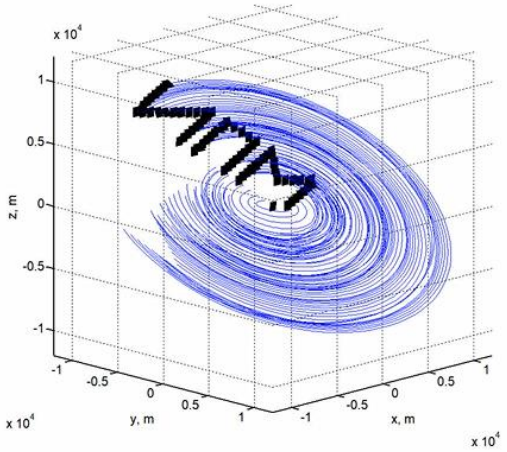

Figure 3. Relative trajectories of satellites with sun-reflectors

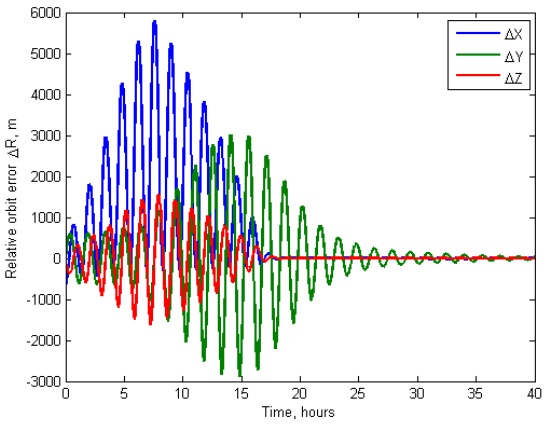

Figure 4. Satellite position vector deviation relative to the last-launched satellite

3.2. Lyapunov-based control

Consider a problem of required relative motion construction of two satellites with solar sails using solar radiation pressure according model (5). Changing the attitude relative to the Sun direction the required forces can be applied using centralized control approach. Consider the following Lyapunov-candidate function:

$$V = \frac{1}{2}C_1^2 + \frac{1}{2}\left(B - B_0\right)^2 + \frac{1}{2}D^2$$

where $B = \sqrt{C_2^2 + C_3^2}$, $D = -3C_1\omega t + C_4$. Value B determine the size of the ellipse in the orbital plane, B_0 is the required size of the ellipse. The conditions $V > 0,\ V(0) = 0$ are satisfied. The derivative of the Lyapunov function should be negative to satisfy the Barbashin-Krasovskii theorem [55] to achieve the global asymptotical stability. The function is constructed in order to eliminate the relative drift C_1, set to zero the relative shift C_4 and achive the required trajectory shape. Lyapunov function time derivative

$$\dot{V} = \frac{1}{\omega}\left(C_1 - 2\left(B - B_0\right)\sin\psi_1\right)u_x + \frac{1}{\omega}\left(\left(B - B_0\right)\cos\psi_1 - 2D\right)u_z - 3C_1 D\omega.$$

where $\psi_1 = \omega t + \beta_1$, β_1 is the initial phase. Then the control is

$$\begin{aligned} u_x &= -k_x\left(C_1 - 2\left(B - B_0\right)\sin\psi_1\right),\ k_x > 0 \\ u_z &= -k_z\left(\left(B - B_0\right)\cos\psi_1 - 2D\right),\ k_z > 0 \end{aligned} \qquad (15)$$

The control algorithm is applied to the problem of constructing the relative motion of two satellites with solar sails taking into account restrictions on the value and direction of the solar radiation force [56]. In Figure 5 the relative orbit is shown. In Figures 5 the blue lines show relative in-plane motion

over the whole control interval while the red lines illustrate resulting relative in-plane motion. The relative trajectory is converged to the required relative trajectory. Figure 6 shows the relative shift and drift that are tending to zero.

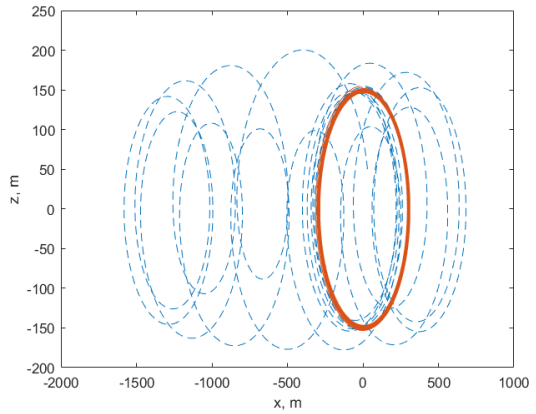

Figure 5. Relative in-plane motion evolution

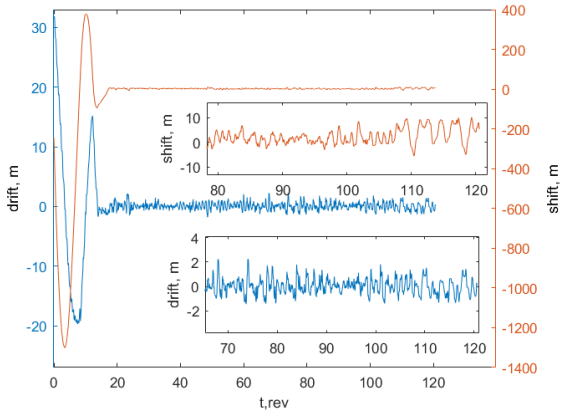

Figure 6. Relative drift and shift

Consider a problem of 3U CubeSat swarm construction after the launch using differential drag using decentralized approach. Their form-factor is suitable for the aerodynamic differential drag control since the ratio of the satellite maximum to minimum cross-section areas is 3. Each satellite is provided with the information about the relative motion of neighboring satellites inside a specified communication area.

Swarm-type flight typically requires only bounded relative motion with no other restrictions. The advantages of random relative trajectories in the swarm are the economy of the control source of the satellites, reduced dependence on the failure of the specific satellite and soft demands for the onboard hardware and software.

The control goal is to construct and maintain a swarm of satellites eliminating their relative drift and limiting the relative trajectories. The shape and size of relative trajectories are determined by the values C^{ij} from (2). Henceforth the constant values C^{ij} of the free relative motion are considered as changing for the controlled motion equations. In order to maintain the satellite motion in the required area it is necessary to adjust the position of the centers of instantaneous ellipses corresponding to the current relative trajectories. From the motion equations (2) it is concluded that the constants C_1^{ij} are responsible for the drift, and the constants C_4^{ij} are responsible for the shift of the centers of the instant ellipses. The control is aimed to maintain the values C_4^{ij} in the vicinity of the required values $\tilde{C}_4^{ij}$ and to eliminate the relative drift C_1^{ij}. The following Lyapunov candidate function is constructed:

$$V = \frac{1}{2}(C_1^{ij})^2 + \frac{1}{2}(\Delta C_4^{ij})^2, \tag{16}$$

where $\Delta C_4^{ij} = \tilde{C}_4^{ij} - C_4^{ij}$. The conditions $V > 0$, $V(0) = 0$ are satisfied. The derivative of the Lyapunov function should be negative to satisfy the Barbashin-Krasovskii theorem [55] to achieve the global asymptotical stability. The derivative is as follows:

$$\dot{V} = C_1^{ij}\dot{C}_1^{ij} + \Delta C_4^{ij}\Delta\dot{C}_4^{ij} = C_1^{ij}\left(\frac{\ddot{x}^{ij}}{\omega} + 2\dot{z}^{ij}\right) + \Delta C_4^{ij}\left(-\dot{x}^{ij} + \frac{2\ddot{z}^{ij}}{\omega}\right). \tag{17}$$

Substitute $\ddot{z}$ from (1) and obtain following derivative expression:

$$\dot{V} = \frac{1}{\omega} C_1^{ij} (\ddot{x}^{ij} + 2\omega \dot{z}^{ij}) + \Delta C_4^{ij} \left(-\dot{x}^{ij} + \frac{2}{\omega} \left(2\omega \dot{x}^{ij} + 3\omega^2 z^{ij} \right) \right) = \frac{1}{\omega} C_1^{ij} u_x + \Delta C_4^{ij} (3\omega C_1^{ij}) . \quad (18)$$

Regroup the expression and demand that Lyapunov function be a definite negative function

$$\dot{V} = C_1^{ij} \frac{1}{\omega} \left(u_x + 3\omega^2 \Delta C_4^{ij} \right) = -\frac{k}{\omega} \left(C_1^{ij} \right)^2 \quad (19)$$

where $k > 0$. The resulting control law is

$$u^{ij} = -kC_1^{ij} - 3\omega^2 \Delta C_4^{ij} . \quad (20)$$

The control u_{ij} provides a convergence to a closed relative trajectory lying in a certain area defined by the value $\tilde{C}_4^{ij}$. The developed control law (20) is similar to the PD controller. The proportional part is the relative shift of instant centers of ellipse C_4^{ij}. Its derivative is proportional to the relative drift value C_1^{ij}.

For decentralized application of the (20) one can calculate the mean value of the deviations for the relative shift and drift. For the i-th satellite with the number of satellites in the communication sphere N_{comm}, which relative motion is known, the average $\bar{C}_1^i, \bar{C}_4^i$ is determined as follows:

$$\bar{C}_4^i = \sum_{j=1}^{N_{comm}} C_4^{ij} / N_{comm}, \; i \neq j. \; \bar{C}_1^i = \sum_{j=1}^{N_{comm}} C_1^{ij} / N_{comm}, \; i \neq j. \quad (21)$$

The example of the proposed strategies is applied to swarm construction consisting of 20 3U CubeSats [57]. Figure 7 demonstrates the trajectories during the first two revolutions and Figure 8 shows the trajectories for the last two revolutions. After the cluster launch the trajectories are diverging from the vicinity of zero as can be seen from Figure 7. Then the trajectories gradually become close to the circular and their centers converge to the origin of the reference frame. However, disturbances, the collision avoidance control and control execution errors induce seldom considerable deviations of the instant centers of trajectories from the origin as it can be seen from Figure 9. Figure 9 provides the change in values $\bar{C}_4^i$ calculated at the time of the control implementation. The individual mean shifts remain nearly constant over time. Figure 10 presents the real relative shifts values C_4^{ij} with respect to the satellite number one (the first to be launched). From Figure 8 one can see that after the launch the relative shifts C_4^i increase due to the launch velocity errors.

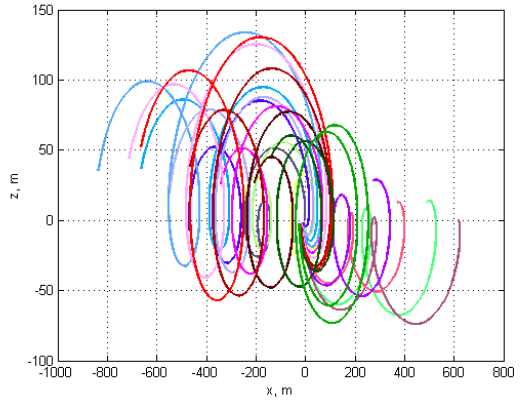

Figure 7. Relative motion trajectories during the first two revolutions

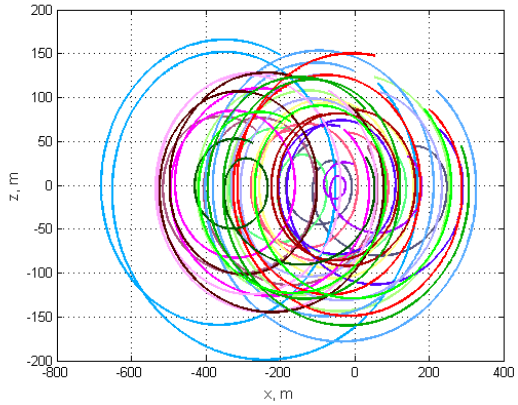

Figure 8. Relative motion trajectories during the last two revolutions

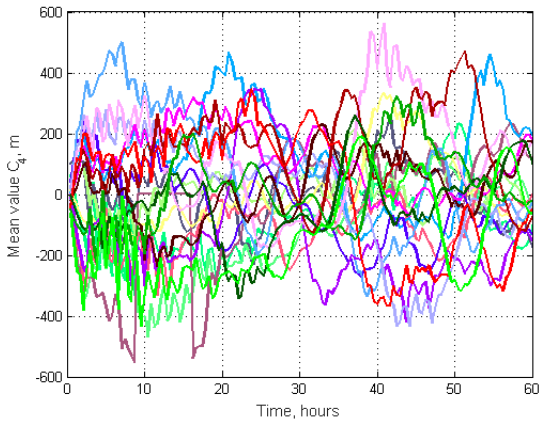

Figure 9. Values of $\overline{C}_4^i$ for all satellites

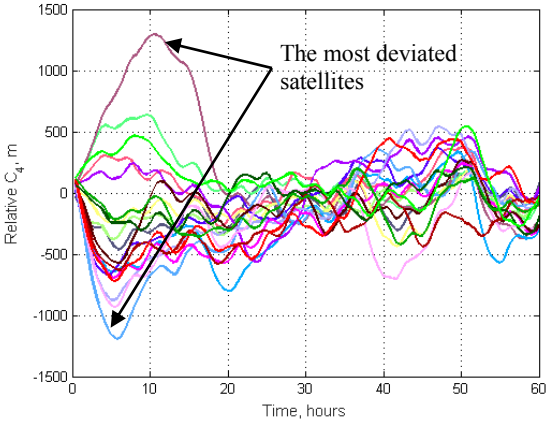

Figure 10. Values C_4 relative to the first launched satellite

Overall, the proposed control successfully maintains the required swarm configuration. The accuracy is mainly governed by the collision avoidance control. The goal of the swarm maintenance control is to reduce mean shifts to zero. However, as the satellite trajectories get closer to each other, the collision danger becomes more frequent and the control is switched to the collision avoidance. The latter is essentially the swarm enlargement one. This contradiction in the control strategies settles the swarm at about 500m distance.

4. Conclusions

The paper reviews a different nanosatellite control approaches using environmental forces. A set of demonstrations of two types of control algorithms applied by the authors are presented. For LQR and Lyapunov-based control algorithms the centralized and decentralized approaches are implemented and difference between them are emphasized. The decentralized approach applied to the swarm control take into account the communicational constraints.

Acknowledgments

The work is supported by the Russian Foundation of Basic Research, grant № 18-31-20014.

References

[1] Alfriend K, Vadali S, Gurfil P, How J and Breger L 2010 *Spacecraft formation flying : dynamics, control and navigation* (Elsevier/Butterworth-Heinemann)

[2] Scharf D P, Hadaegh F Y and Ploen S R A survey of spacecraft formation flying guidance and control (part 1): guidance *Proceedings of the 2003 American Control Conference, 2003.* vol 2 (IEEE) pp 1733–9

[3] Di Mauro G, Lawn M and Bevilacqua R 2018 Survey on Guidance Navigation and Control Requirements for Spacecraft Formation-Flying Missions *Journal of Guidance, Control, and Dynamics* **41** 581–602

[4] Kumar K D, Misra A K, Varma S, Reid T and Bellefeuille F 2014 Maintenance of satellite formations using environmental forces *Acta Astronautica* **102** 341–54

[5] Leonard C L, Hollister W M and Bergmann E V 1989 Orbital formationkeeping with differential drag *Journal of Guidance, Control, and Dynamics* **12** 108–13

[6] Kumar B S and Ng A 2008 A bang-bang control approach to maneuver spacecraft in a formation with differential drag *Proceedings of the AIAA Guidance, Navigation and Control Conference and Exhibit, 18-21 August 2008, Honolulu, Hawaii* AIAA 2008-6469

[7] Zeng G, Ru M and Yao R 2012 Relative orbit estimation and formation keeping control of satellite formations in low Earth orbits *Acta Astronautica* **76** 164–75
[8] Varma S and Kumar K D 2012 Multiple Satellite Formation Flying Using Differential Aerodynamic Drag *Journal of Spacecraft and Rockets* **49** 325–36
[9] Omar S R and Wersinger J M 2015 Satellite Formation Control using Differential Drag *53rd AIAA Aerospace Sciences Meeting* 1–11
[10] Gong S, Yunfeng G and Li J 2011 Solar sail formation flying on an inclined Earth orbit *Acta Astronautica* **68** 226–39
[11] Shahid K and Kumar K D 2014 Multiple spacecraft formation reconfiguration using solar radiation pressure *Acta Astronautica* **103** 269–81
[12] Shahid K and Kumar K D 2010 Formation Control at the Sun-Earth L(2) Libration Point Using Solar Radiation Pressure *Journal of Spacecraft and Rockets* **47** 614–26
[13] Gong S, Baoyin H and Li J 2007 Solar Sail Formation Flying Around Displaced Solar Orbits *Journal of Guidance, Control, and Dynamics* **30** 1148–52
[14] Williams T and Wang Z-S 2002 Solat Radiation Pressure and Formation-Keeping in Highly Elliptical Orbits *AIAA/AAS Astrodynamics Specialist Conference and Exhibit* pp 1–14
[15] King L B and Parker G G 2002 Spacecraft Formation-flying using Inter-vehicle Coulomb Forces 1–103
[16] Mullen E G, Gussenhoven M S and Hardy D A 1986 SCATHA Survey of High-Voltage Spacecraft Charging in Sunlight *Journal of the Geophysical Sciences* **91** 1074–90
[17] Felicetti L and Palmerini G B 2016 Analytical and numerical investigations on spacecraft formation control by using electrostatic forces *Acta Astronautica* **123** 455–69
[18] Felicetti L and Palmerini G B 2016 Three spacecraft formation control by means of electrostatic forces *Aerospace Science and Technology* **48** 261–71
[19] Inampudi R and Schaub H 2010 Optimal Reconfigurations of Two-Craft Coulomb Formation in Circular Orbits *Proceedings of the AIAA Guidance, Navigation, and Control Conference* **35**
[20] Saaj C M, Lappas V, Schaub H and Izzo D 2010 Hybrid propulsion system for formation flying using electrostatic forces *Aerospace Science and Technology* **14** 348–55
[21] Hogan E A and Schaub H 2012 Collinear invariant shapes for three-spacecraft Coulomb formations *Acta Astronautica* **72** 78–89
[22] Inampudi R and Schaub H 2014 Orbit Radial Dynamic Analysis of Two-Craft Coulomb Formation at Libration Points *Journal of Guidance, Control, and Dynamics* **37** 682–91
[23] Hogan E A and Schaub H 2012 Relative motion control for two-spacecraft electrostatic orbit corrections *Advances in the Astronautical Sciences* **142** 967–86
[24] Schaub H and Jasper L E Z 2013 Orbit Boosting Maneuvers for Two-Craft Coulomb Formations *Journal of Guidance, Control, and Dynamics* **36** 74–82
[25] Jasch P D, Hogan E A and Schaub H 2012 Stability analysis and out-of-plane control of collinear spinning three-craft Coulomb formations *Advances in the Astronautical Sciences* **143** 747–62
[26] Jones D R and Schaub H 2014 Collinear Three-Craft Coulomb Formation Stability Analysis and Control *Journal of Guidance, Control, and Dynamics* **37** 224–32
[27] Anon *Schweighart, S. A., "Electromagnetic Formation Flight—Dipole Solution Planning," Ph.D. Thesis, Massachusetts Inst. of Technology, June 2005.*
[28] Hallaj M A A and Assadian N 2016 Sliding mode control of electromagnetic tethered satellite formation *Advances in Space Research* **58** 619–34
[29] Schweighart S A and Sedwick R J 2006 Propellantless Formation Flight Operations using Electromagnetic Formation Flight *AIAA 2006-5579, SpaceOps Conference*
[30] Zeng G and Hu M 2012 Finite-time control for electromagnetic satellite formations *Acta Astronautica* **74** 120–30
[31] Huang H, Zhu Y W, Yang L P and Zhang Y W 2014 Stability and shape analysis of relative equilibrium for three-spacecraft electromagnetic formation *Acta Astronautica* **94** 116–31

[32] Miller D W, Ahsun U and Ramirez-Riberos J L 2010 Control of Electromagnetic Satellite Formations in Near-Earth Orbits *Journal of Guidance, Control, and Dynamics* **33** 1883–91
[33] Elias L M, Kwon D W, Sedwick R J and Miller D W 2007 Electromagnetic Formation Flight Dynamics Including Reaction Wheel Gyroscopic Stiffening Effects *Journal of Guidance, Control, and Dynamics* **30** 499–511
[34] Kwon D W, Sedwick R J, Lee S-I and Ramirez-Riberos J 2011 Electromagnetic Formation Flight Testbed Using Superconducting Coils *Journal of Spacecraft and Rockets* **48** 124–34
[35] Peck M A, Streetmani B, Saaj C M and Lappas V 2007 Spacecrat Formation Flying Using Lorentz Forces *Journal of the British Interplanetary Society* **60** 263–7
[36] Huang X, Yan Y and Zhou Y 2015 Analytical solutions to optimal underactuated spacecraft formation reconfiguration *Advances in Space Research* **56** 2151–66
[37] Tsujii S, Bando M and Yamakawa H 2013 Spacecraft Formation Flying Dynamics and Control Using the Geomagnetic Lorentz Force *Journal of Guidance, Control, and Dynamics* **36** 136–48
[38] Chung S-J and Miller D W 2008 Propellant-Free Control of Tethered Formation Flight, Part 1: Linear Control and Experimentation *Journal of Guidance, Control, and Dynamics* **31** 571–84
[39] Zhang J, Yang K and Qi R 2018 Dynamics and offset control of tethered space-tug system *Acta Astronautica* **142** 232–52
[40] Chen Y, Huang R, Ren X, He L and He Y 2013 History of the Tether Concept and Tether Missions: A Review *ISRN Astronomy and Astrophysics* **2013** 1–7
[41] Guerman A D, Smirnov G, Paglione P and Vale Seabra A M 2008 Stationary Configurations of a Tetrahedral Tethered Satellite Formation *Journal of Guidance, Control, and Dynamics* **31** 424–8
[42] Gates S S, Koss S M and Zedd M F 2001 Advanced Tether Experiment Deployment Failure *Journal of Spacecraft and Rockets* **38** 60–8
[43] Tragesser S G 2009 Static Formations Using Momentum Exchange Between Satellites *Journal of Guidance, Control, and Dynamics* **32** 1277–86
[44] Ketsdever A and Schonig J A 2012 Constant Momentum Exchange to Maintain Spacecraft Formations *Journal of Spacecraft and Rockets* **49** 69–75
[45] Defense C and Ground A P 2005 Report Documentation Page *System* **298**
[46] Ivanov D, Ovchinnikov M and Shestakov S 2014 Satellite formation flying control by mass exchange *Acta Astronautica* **102** 392–401
[47] Kumar B S, Ng A and Bang-Bang A Control Approach to Maneuver Spacecraft in a Formation With Differential Drag *Proceedings of the AIAA Guidance, Navigation and Control Conferenceand Exhibit, AIAA Paper No.2008-6469, Honolulu, Hawaii, August 2008.*
[48] Ivanov D, Kushniruk M and Ovchinnikov M 2018 Study of satellite formation flying control using differential lift and drag *Acta Astronautica* **145** 88–100
[49] Pérez D and Bevilacqua R 2014 Lyapunov-Based Adaptive Feedback for Spacecraft Planar Relative Maneuvering via Differential Drag *Journal of Guidance, Control, and Dynamics* **37** 1678–84
[50] Pérez D and Bevilacqua R 2013 Differential drag spacecraft rendezvous using an adaptive Lyapunov control strategy *Acta Astronautica* **83** 196–207
[51] Kumar K D, Misra A K, Varma S and Bellefeuille F 2014 Maintenance of Satellite Formations Using Environmental Forces *Acta Astronautica* **102** 341–54
[52] Dellelce L and Kerschen G 2015 Optimal propellantless rendez-vous using differential drag *Acta Astronautica* **109** 112–23
[53] Ovchinnikov M Y, Ivanov D S, Ivlev N a., Karpenko S O, Roldugin D S and Tkachev S S 2014 Development, integrated investigation, laboratory and in-flight testing of Chibis-M microsatellite ADCS *Acta Astronautica* **93** 23–33
[54] Ciarci M, Grompone A and Romano M 2014 A near-optimal guidance for cooperative docking maneuvers *Acta Astronautica* **102** 367–77

[55] Barbashin E A 1961 On construction of Lyapunov functions for non- linear systems *Proc. First Congr. IFAK, Moscow* pp 742– 751
[56] Mashtakov Y, Ovchinnikov M, Petrova T and Tkachev S 2020 Two-satellite formation flying control by cell-structured solar sail *Acta Astronautica* **170** 592–600
[57] Ivanov D, Monakhova U, Guerman A, Ovchinnikov M and Roldugin D 2020 Decentralized differential drag based control of nanosatellites swarm spatial distribution using magnetorquers *Advances in Space Research*